Macromolecules

Article

pubs.acs.org/Macromolecules

# Geometric and Edge Effects on Swelling-Induced Ordered Structure Formation in Polyelectrolyte Hydrogels

Md. Arifuzzaman,[†] Zi Liang Wu,[‡,§] Riku Takahashi,[†] Takayuki Kurokawa,[‡] Tasuku Nakajima,[‡] and Jian Ping Gong[‡,*]

[†]Laboratory of Soft and Wet Matter, Division of Biological Sciences, Graduate School of Science, Hokkaido University, Sapporo 060-0810, Japan

[‡]Laboratory of Soft and Wet Matter, Division of Life Sciences, Faculty of Advanced Life Science, Hokkaido University, Sapporo 060-0810, Japan

Supporting Information

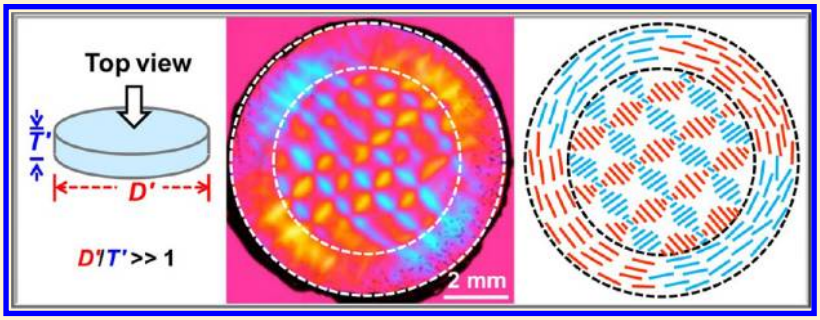


**ABSTRACT:** In this paper, we developed several kinds of ordered structures in hydrogels with different geometries and sizes by harnessing heterogeneous swelling induced mechanical instability, i.e., surface creasing, which leads to molecular orientations along the tensile direction. These hydrogels were synthesized by polymerization of a cationic monomer, *N*-[3-(*N*,*N*-dimethylamino)propyl] acrylamide methyl chloride quaternary (DMAPAA-Q) and a chemical cross-linker, in the presence of a small amount of the *semirigid* polyanion, poly(2,2′-disulfonyl-4,4′-benzidine terephthalamide) (PBDT), as dopant. During the swelling process of as-prepared gels, surface creasing occurs and induces formation of a lattice-like periodic ordered structure, which is maintained in the swollen gels due to the formation of strong polyion complex. Besides this structure formed at the central part of gel sheets, PBDTs align parallel to the gel boundary at the edge of gels with a cuboid, disk, or ring shape. The size of the two regions with different structures and the size of each unit of lattice-like pattern are related to the geometry and size of the gels. The formation of different ordered structures was found due to the different mechanical instabilities at different parts of the gel during the heterogeneous swelling. This work presenting the creation of ordered structures in hydrogels by tuning the mechanical instability will pave the way to develop other functional structured materials and merit revealing the formation mechanism of ordered structures in soft biotissues during the nonequilibrium growth.

## INTRODUCTION

Natural living organisms are full of intriguing topographical patterns,[1,2] such as bumps on the surface of the primate brain,[3] intense waves on the finger tip after immersion into water for prolonged period of time,[4] wrinkles on the skin of human beings, fruits, or vegetables, etc.[5−8] Nonequilibrium growing processes of living soft tissues beneath the outermost surface or mismatched deformations between "shell" (skin of the fruit or membrane of the cell) and underlying "core" (flesh of the fruit or cytoplasm of the cell) develop internal stresses that cause the surfaces of these living bodies to undulate, buckle, or fold.[7−12] Human fingerprint patterns result from the buckling of the layer of basal cells of the fetal epidermis.[8] Long leaf of *Antirrhinum* has a wavy surface with buckled margins, which stems from the spontaneous buckling driven by the in-plane differential growth in the leaf.[7,11] These mechanical instabilities during the inhomogeneous growth or change of the states of the soft tissues play a crucial role in regulating pattern formation and morphogenesis of tissues and organs.

With inspiration from nature, there have been growing interests in designing soft materials with controllable deformations of the integrated or part of materials, such as buckled surfaces, by controlling the mechanical instabilities and internal/residual stresses. Hydrogels, a typical soft and wet material, also manifest various kinds of surface patterns upon swelling or shrinking induced instability.[13−23] If the gel is unconstrained and has a uniform network structure, the mechanical instability and surface patterns will gradually disappear as the entire gel achieves a swelling equilibrium state. Two general ways are applied to develop a stable period

**Received:** August 23, 2013
**Revised:** October 31, 2013
**Published:** November 12, 2013

  

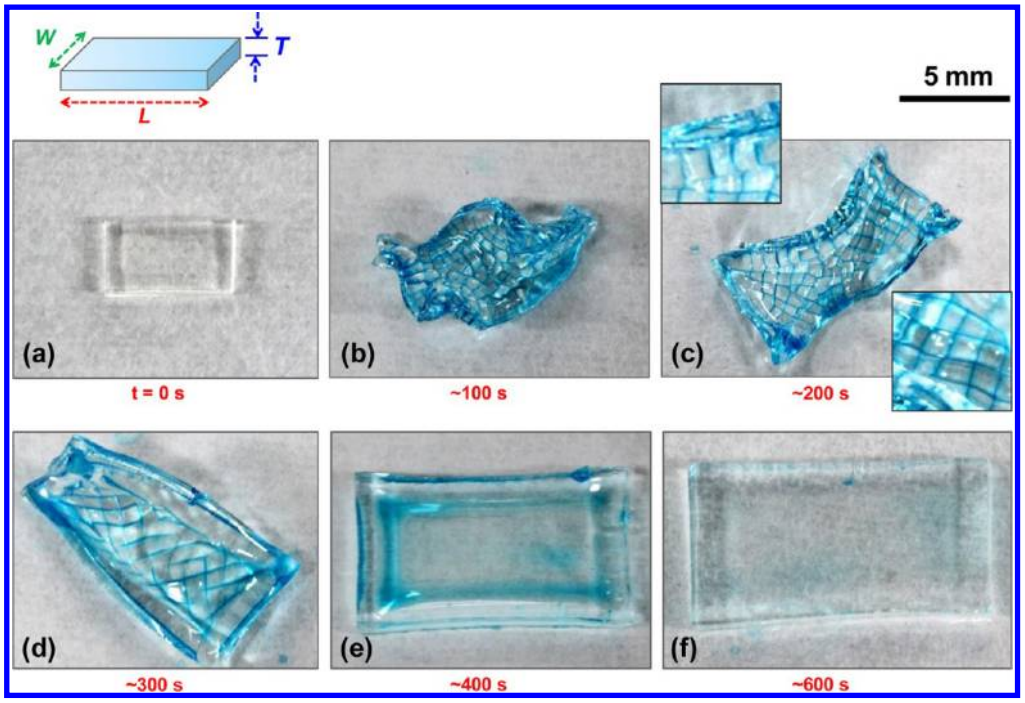


**Figure 1.** Surface instability pattern evolution of the cuboid shape polyelectrolyte PDMAPAA-Q hydrogel due to the strong surface instability during free-fast-heterogeneous swelling process. To observe clearly the boundary of surface pattern, the as-prepared hydrogel was swollen in water containing 0.05 wt % Alcian blue. Insets are parts of the image in part c showing clearly the surface pattern at the edge and the center of the gel. All the images are shown in the same scale as shown in the above of part c. The dimension of the as-prepared gel was about 6 mm ($L$) × 3 mm ($W$) × 1.0 mm ($T$). Swelling ratio in length, $q$, of the gel is ~2.2. In the absence of Alcian blue, we observed exactly the same surface instability patterns.

surface pattern: (i) to produce gradient in modulus or cross-linking density within the hydrogel,[15,18,22] (ii) to let the gel expand or contract in a constrained space.[13,14,17,19] For example, Kim et al. have fabricated responsive patterned creases of the gel which was bound to a solid patterned substrate; swelling of the gel in a constrained space, which was controllable by the substrate pattern, produced elastic creasing instability and a period buckled surface.[19] Under the transient or stable creasing/buckling, the local regions of the gel was severely stretched or compressed,[6] which should lead to molecular orientation to some extent.

Stress/strain induced molecular alignments of polymer chain or network are widely investigated in biotissues, elastomers, gels, and plastics.[24−29] For example, cellulose and pectin had little orientation in native epidermal cell wall; however, they showed distinct orientation when the cell was stretched.[24] Urayama et al. found that under a small stretch strain, $\varepsilon \sim 0.3$, the mesogens of liquid crystalline elastomers realigned along the stretching axis from their pristine homeotropic alignment.[29] If the molecular orientation is sensitive to a complex internal stress field that is controllable throughout the soft materials, biomimetic structured materials with different molecular alignments could be expected, which is still challenging at this date. The transient or stable, well-distributed stress could be realized in hydogels by tuning the localized internal stress or mechanical instability.[30,31,19] However, to the best of our knowledge, the formation of stable, periodic structure of molecular alignments in the hydrogel by harnessing mechanical instabilities has not been investigated so far.

Recently, we have found that the mechanical instability developed during fast-heterogeneous swelling of a hydrogel can be used to form ordered structure of semirigid molecules.[32] The hydrogel was synthesized by polymerization of a cationic monomer, *N*-[3-(*N*,*N*-dimethylamino)propyl] acrylamide methyl chloride quaternary (DMAPAA-Q), and a chemical cross-linker, in the presence of a small amount of the semirigid polyanion, poly(2,2′-disulfonyl-4,4′-benzidine terephthalamide) (PBDT), as the dopant. After a heterogeneous swelling, which induces strong surface creasing/buckling instability, periodic structures with oriented PBDTs are produced in the hydrogel film. The significant mismatch of swelling degree between the outer and inner part of hydrogel builts internal stress, leading to orientation of the dopant semirigid polyanion along the tensile direction of the buckled surface. Interestingly, in accompany with the evolution of surface instability pattern, a lattice-like periodic birefringence pattern appears, which is permanently frozen by the strong polyion complexation between the positively charged poly(DMAPAA-Q) (PDMAPAA-Q) network and the negatively charged semirigid PBDT. The ordered structure of the gel was found extremely stable even after the swelling mismatch and surface instability disappeared completely.

In this paper, we systematically studied the geometric effects on the molecular alignments within hydrogels induced by the fast heterogeneous swelling and buckling instabilities. As-prepared PBDT containing PDMAPAA-Q hydrogels were cut into different shapes and sizes and then swelled in a large amount of water. We found that the edge parts of the swollen gels showed different birefringence pattern from that at the central part. As we reported before, a lattice-like periodic birefringence pattern formed at the central part. However, a uniform birefringence, corresponding to unidirectional alignment of molecules (in disc or ring-shaped gels, molecular alignments are along with their boundary), formed at the edge part of gels. The difference originated from the different mechanical instabilities at different parts of the gel during the occurrence of heterogeneous swelling. The size of the lattice-like periodic structure at the central part and the width of edge part with


dx.doi.org/10.1021/ma401773w | *Macromolecules* 2013, 46, 9083−9090

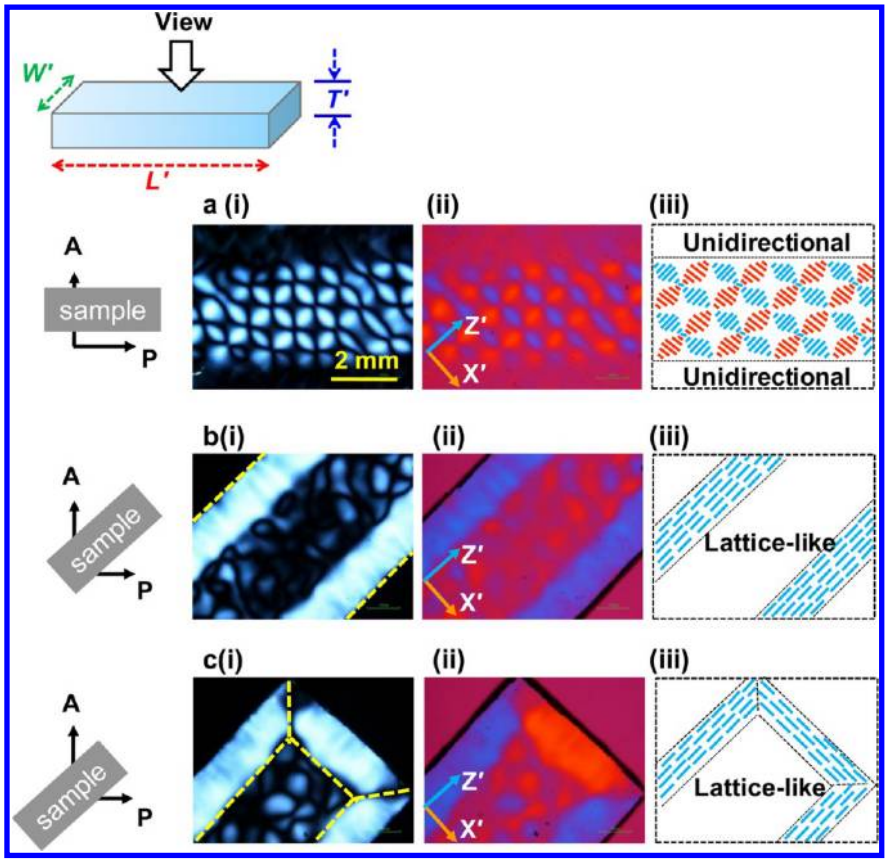


**Figure 2.** Ordered birefringent pattern and corresponding orientation of PBDT molecules formed in a PDMAPAA-Q hydrogel film after a fast-heterogeneous swelling process. The polarizing optical microscope (POM) images of the gel are observed at different position and azimuth under crossed polarizers (i) and with insertion of 530 nm tint plate (ii). Illustrations in column iii indicate the PBDT molecular orientation in the hydrogel. (a, b) Central part of gel placed parallel (a) and 45° to the direction of polarizer (b). (c) End part of gel placed 45° to the direction of polarizer. The dimension of the as-prepared gel was about 6 mm ($L$) × 3 mm ($W$) × 1.0 mm ($T$). Swelling ratio in length, $q$, of the gels is ~2.2. All the images have the same scale bar, as shown in part a(i). Key: A, analyzer; P, polarizer, $X'$ and $Z'$, fast and slow axis of the tint plate, respectively.

uniform alignment only depend on the gel thickness, regardless of other geometric parameters of the gel. The robust method permits us to develop hydrogels with complex ordered structures of molecular alignments and should merit designing structured hydrogels by controlling mechanical instabilities. The abilities of rigid macromolecules to sensitively "detect" and "remember" the stress state through locked-in orientations of the liquid crystal molecules also have a potential to analyze the internal stress field of the soft materials.

## EXPERIMENTAL SECTION

**Materials.** PBDT, a water-soluble anionic semirigid polymer, was synthesized by an interfacial polycondensation reaction.[33,34] The weight-average molecular weight, $M_w$ of the synthesized PBDT was $1.6 \times 10^6$ g/mol. Its aqueous solutions showed a critical low liquid crystalline concentration, $C_{LC}$* of 2.8 wt %.[34−36] The cationic monomer, DMAPAA-Q (Kohjin Co. Ltd. Japan), the photoinitiator, 2-oxoglutaric acid (OA) (Wako Pure Chemical Industries Ltd.) were used as received without further purification. *N*,*N*′-Methylenebis-(acrylamide) (MBAA) (Wako Pure Chemical Industries Ltd. Japan) was recrystallized from ethanol and used as a chemical cross-linker. For all the experiments, water was deionized and purified with 0.22 and 5 μm membrane filter prior to use.

**Preparation of PBDT Containing PDMAPAA-Q Gel with Different Shapes and Sizes.** To synthesize hydrogel film, the reaction cells were prepared by sandwiching the square frame of a silicone spacer with different thickness between the two parallel glass plates. The aqueous pregel solutions, containing 1 wt % of PBDT (dopant semirigid polyanion), 2 M of DMAPAA-Q (the cationic monomer), 2 mol % (relative to the amount of monomer) of MBAA (the chemical cross-linker, and 0.15 mol % (relative to the amount of monomer) of OA (the initiator), was injected into the reaction cells. As-prepared gels were obtained after UV irradiation from the both sides of the reaction cell for 6 h under an argon atmosphere.

The as-prepared gel films were cut into desired shapes and sizes by using a mechanical gel cutter (Dumbbell Co. Ltd., Japan). As-prepared gels with three types of shapes were prepared in current work: cuboid shape (length, $L$; width, $W$; thickness, $T$), disk shape (diameter, $D$; thickness, $T$), and ring shape (outer diameter, $D_0$; inner diameter, $D_i$; thickness, $T$). The dimensions of the swollen gels are: $L' \times W' \times T'$ (length × width × thickness) for cuboid gel, $D' \times T'$ (diameter × thickness) for disk gel, and $(D_0' - D_i') \times T'$ ((outer diameter − inner diameter) × thickness) for ring gel.

**Swelling Experiments of the Polyelectrolyte Gel.** The as-prepared gels with different shapes and sizes were swelled in a large amount of water. The gel achieved equilibrium state after a fast heterogeneous swelling. The swelling ratio in length, $q$, is obtained by calculating the ratio between the dimensions of swollen gel and those of as-prepared gel.

To observe the swelling induced surface instability pattern formation and its evolution, the as-prepared gel with a cuboid shape was immersed into aqueous dye solution with 0.05 wt % Alcian blue. At different swelling time, the gel was taken out from the solution to take a picture. Owing to the surface tension force of liquid, the dye solution was left to some extent around the creasing lines, so that the surface creasing/buckling lines and patterns were visualized.

**Polarizing Optical Microscope (POM) Observation.** Birefringence of PBDT-containing PDMAPAA-Q gel, including irregular birefringence in the as-prepared state and mesoscale periodic ordered


dx.doi.org/10.1021/ma401773w | *Macromolecules* 2013, 46, 9083−9090

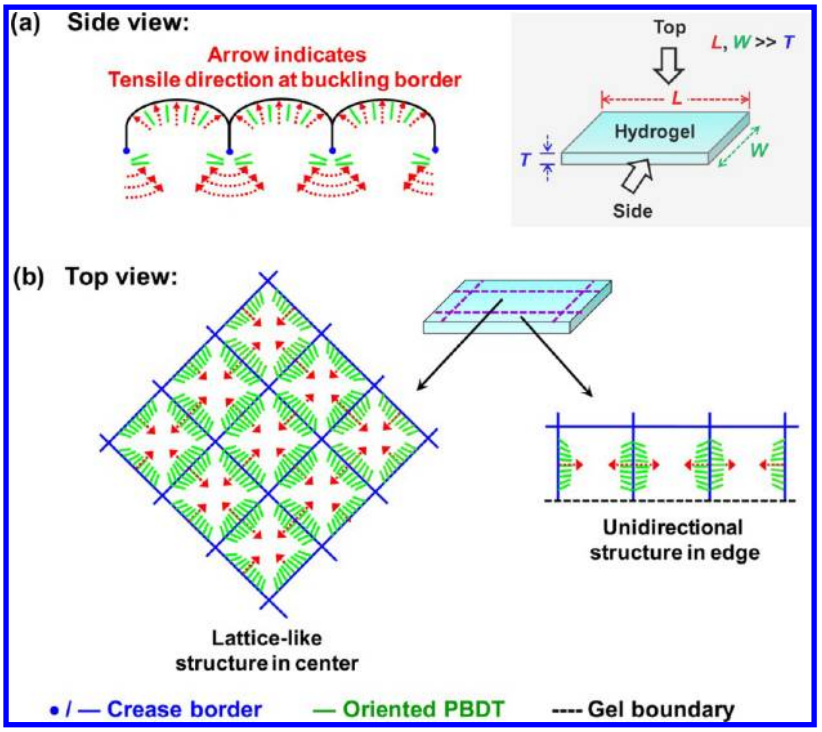


**Figure 3.** Schematic for ordered/periodic pattern and molecular orientation in a cuboid shaped PBDT-containing PDMAPAA-Q hydrogel film formed under heterogeneous swelling induced internal stress field. Subsequently, the ordered structure of PBDTs is frozen by the strong polyion complexation between the two oppositely charged polymers. Part a shows side view of surface instability buckling pattern, which exerts tensile stress vertical to the boundary of each buckling unit and induces macromolecular orientation. Part b shows top view of different surface instability patterns along with different ordered PBDT orientations at different region of the gel. The internal stress field induced by heterogeneous swelling (outer layer of gel swells faster than that of inner part) is completely different at the edge compared to the central region of the hydrogel, leading to different surface buckling pattern and thus different PBDT orientations frozen in the gel.

birefringence after the completion of swelling, were observed at room temperature under the crossed polarizing optical microscope (POM) (Nikon, Eclipse LV100POL). Sample gels were placed on glass slides and observed from the top. All the samples with different shapes and sizes exhibited a first order white-gray birefringence color, so that a 530 nm sensitive tint plate was inserted to distinguish the orientations of the semirigid PBDT.[37−39]

## RESULTS AND DISCUSSION

The internal stress field generation inside the hydrogel is induced by the mechanical instability, therefore it should have strong correlation with the initial shape and size, i.e., the geometry of the hydrogels.[40] During the heterogeneous swelling process, the edge part of hydrogels could absorb water from the top, bottom, and side surfaces, whereas the central part of gel swelled only when the water penetrate through the top and bottom surfaces. Therefore, the internal stress fields at the central and edge of hydrogel should be quite different. These differential internal stresses induce surface patterns and corresponding molecular orientations within the gels.

The evolution of mechanical instability induced surface pattern is observed *in situ* during the free-fast-heterogeneous swelling process. After immersing the as-prepared hydrogels into water, surface creasing/buckling appears in all gels with cuboid or disk shape. The surface of the as-prepared gel with cuboid shape is completely flat, without any type of convolutions (Figure 1a). However, at the initial period of free swelling, numerous convex polygonal bumps on the surface of the gel and sinusoidal large convolution at the edge are clearly observed (Figure 1b). It is worth mentioning that at this stage of swelling, three bumps on the gel surface are fused together in a common junction point (see Supporting Information, Figure S1a). On the basis of the swelling time, a clear change in surface as well as in three-dimensional (3D) hierarchical buckling instability pattern is observed.[31] Interestingly, after around 200 s of swelling, four bumps start to share a common junction point (see Supporting Information, Figure S1b), and thus the surface instability pattern shows an array of lattice-like lines (corresponding to border lines of creases) in the center of gel. Although the entire gel shows almost torsional deformed shape, parallel stripe lines with a regular spacing, which are vertical to the boundary, appear at the edge of gel (Figure 1c). In progress at ∼300 s, as shown in Figure 1d, parallel stripe lines at the edge disappear, indicating the weakening of mechanical instability, whereas the lattice-like lines sustain for longer time. As the heterogeneity of swelling degree decreases, the deformed partially swollen gel recovered to its original cuboid shape (Figure 1e). Finally, all the surface patterns and buckling instability disappear since the internal stress built by the swelling mismatch inside the hydrogel is fully compensated (Figure 1f). At equilibrium swelling state, the gel becomes flat, and the swelling ratio, $q$, in every dimension of the gel with any shapes is approximately 2.2 (see Supporting Information, Figure S2).

The above observation clearly shows that the mechanical instability at the edge of gel is different from that at the central part (Figure 1d). At the beginning of swelling, the edge part of the hydrogel swells faster and achieves equilibrium earlier than the central part due to the different ratio of the surface, which is exposed to water, and the volume of the gel. Therefore, the distribution of internal stress, induced by the mismatch of swelling ratio between the outer swollen region and inner


dx.doi.org/10.1021/ma401773w | *Macromolecules* 2013, 46, 9083−9090

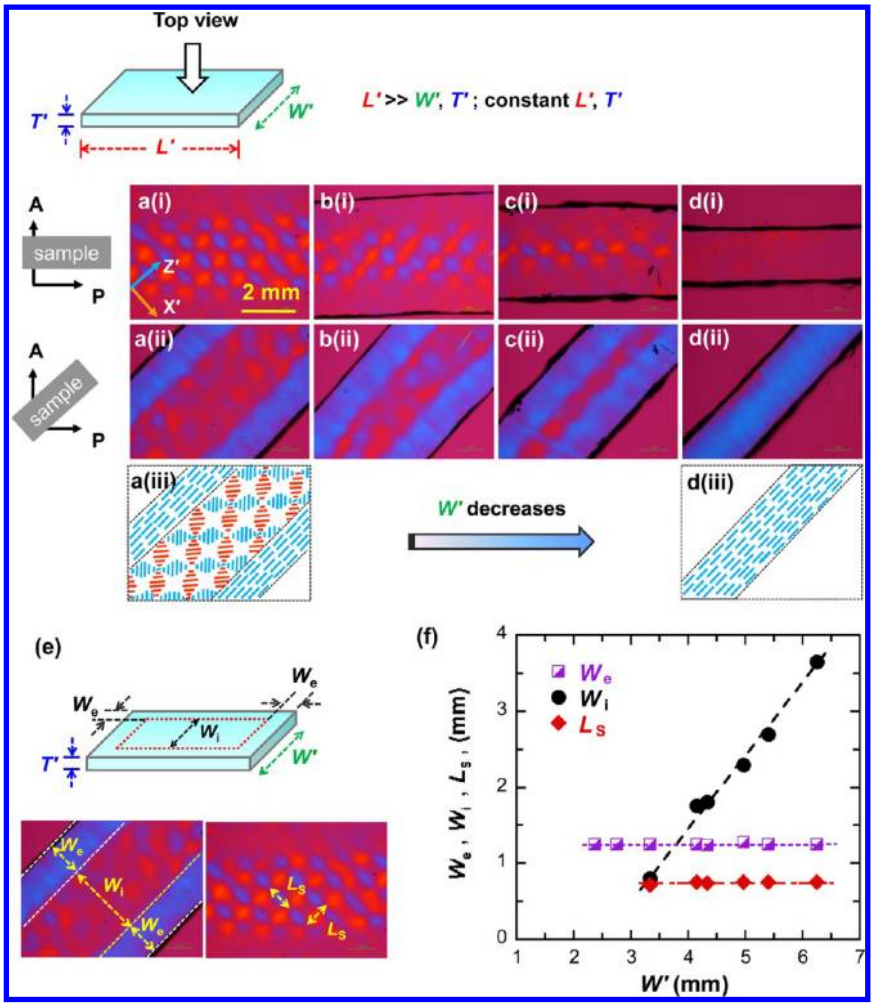


**Figure 4.** (a-d) POM images to show the change of ordered structure as the width of the swollen gel, $W'$, decreases. Central part of gel is placed parallel (i) and 45° to the direction of polarizer (ii) for POM observation. Representative PBDT orientation in the gel was shown in part iii to show the change of ordered structure as $W'$ decreases. The dimensions of the as-prepared gel were about 6 mm ($L$) × $a$ mm ($W$) × 1 mm ($T$), where $a$ ranges from 0.5 to 3 mm. Swelling ratio in length, $q$, of the gel is ~2.2. All the images have the same scale bar, as shown in part a(i). (e) Schematic to show the measurements of the width of unidirectional alignment region at the edge of gel, $W_e$, width of the lattice-like structure in the central region of gel, $W_i$, and size of each lattice-like unit, $L_S$. (f) Variation of $W_e$, $W_i$, and $L_S$ as a function of $W'$.

unswelled region of gel, is largely different in the center and edge part of the gel. Under this heterogeneous internal stress field, mechanical instability leads to different PBDT orientations at the center and edge of the hydrogel. As we illustrated in our previous paper, the internal stress induced molecular orientations could be frozen by the complexation between PBDT and PDMAPAA-Q during the following swelling process,[32] so that we could recall the internal stress during heterogeneous swelling by analyzing the molecular alignment within swollen gels. The POM images from the top of the sample show a uniform birefringence at the edge of the swollen gel, and a lattice-like pattern of birefringence at the central part of gel (Figure 2). According to the birefringent colors of the samples observed under crossed polarizers with insertion of tint plate, we could confirm the alignments of PBDT within the gel.[37−39] The PBDT molecules at the central region are aligned perpendicular to the borderlines of the creases to form a lattice-like pattern, which is identical to that reported before (Figure 2a(iii)). At the edge part of the gel, PBDTs align parallel to the gel boundary. We should note that PBDT alignments parallel to the boundary meet at the corner with a clear demarcation, i.e. the angle bisector of the corner (Figure 2c).

For the gel with cuboid shape, the internal stress is built in the hydrogel by the strong swelling mismatch between the surface and inner hydrogel layers. At the central part of gel, the regions close to two outer surfaces swelled at the initial swelling process, whereas as the inner region is still unswelled. This mechanical instability induces the formation of period lattice-like buckled pattern of the surface (Figure 3a). The semirigid PBDT and its polyion complex are very sensitive to mechanical stress/strain,[24,34] so that PBDTs strongly orient along with the tensile direction, i.e. vertical to the borderlines of the creasing patterns (Figure 3b). On the other hand, the edge of the gel swells faster than that of the central part, because water could also penetrate from the side of the gel, corresponding to the earlier disappearance of buckled lines than the central region. The edge part of the gel could swell freely in the direction vertical to the gel boundary, yet was constrained in the direction along with the boundary due to the direct connection to the central part of gel with a relatively small expansion degree. This internal stress, compression along the gel boundary,[18,41−44] results in buckled surface with borderline vertical to the gel boundary (Figure 1c). Therefore, at the edge part of gel, PBDTs orient vertical to the borderlines, forming a unidirectional


dx.doi.org/10.1021/ma401773w | Macromolecules 2013, 46, 9083−9090

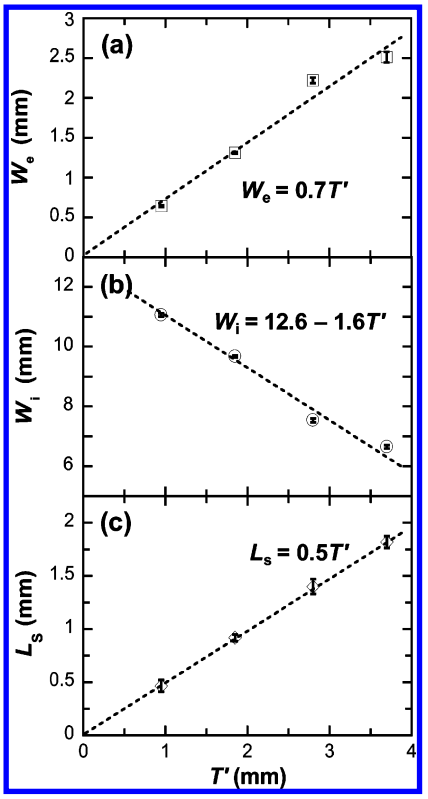


**Figure 5.** Variations of (a) $W_e$, (b) $W_i$, and (c) $L_S$ as a function of the thickness of swollen gel, $T'$. The dimension of the as-prepared cuboid gel was 8 mm ($L$) × 6 mm ($W$) × $b$ mm ($T$), where $b$ is varied from 0.5 to 2 mm. Swelling ratio in length, $q$, of the gel is ∼2.2.

alignment parallel to the gel boundary (Figure 3b). As we stated before, this periodic structure is frozen by the formation of polyion complex, accompanying with the diffusion of counterions out of the gel, and thus could be maintained after the disappearance of mechanical instability.[45,46]

After revealing the formation mechanism of periodic structure, another question is what determines the width of edge region with unidirectional alignment of PBDTs and the size of each unit of lattice-like pattern formed at the central of gel. To address this issue, we systematically changed the dimensions of gels with a cuboid shape. First, we varied the width ($W$) of as-prepared gel, while keeping its length ($L$) and thickness ($T$) constant. After swelling, each dimension becomes ∼2.2 times of its original length. As shown in Figure 4a–d, the width of lattice-like region at the central of the swollen gel gradually decreases and finally disappears as width of swollen gel, $W'$, decreases to 2.5 mm. Then, the widths of central lattice-like region and edge unidirectional alignment region, $W_e$ and $W_i$ (Figure 4e), respectively, and the size of lattice unit, $L_S$, were measured and plotted as a function of $W'$. $W_e$ and $L_S$ keep constant values of 1.25 and 0.75 mm, respectively, whereas $W_i$ increases linearly with $W'$ (Figure 4f). Second, we changed $T'$, while keeping $L'$ and $W'$ constant (as-prepared gels: $L$ = 8 mm, $W$ = 6 mm). As $T'$ increases, $W_e$ and $L_S$ increase ($W_e$ = 0.7$T'$ and $L_s$ = 0.5$T'$, respectively), yet $W_i$ linearly decreases ($W_i$ = 12.6 − 1.6$T'$ ∼ $W'$ − 2$W_e$) (Figure 5). These findings permit us a better control of the oriented domain size in the gels.

All the above experimental results support well the structure formation mechanism we proposed in Figure 3. For example, $W_e$ should correspond to the width of an edge region which is fully swelled, meanwhile the central region is still not. If $T'$ is kept constant, there should be an identical mismatch of swelling between the edge and central of gel and thus a constant $W_e$, which stems from the different speed to swell the local regions of gels. The lattice-like birefringence and ordered molecular structure result from the period buckling pattern, which is induced by the mismatch of swelling between the outer layers and inner region of the gel at the central part of gels. We have investigated the time evolution of the lattice pattern formation in a previous work.[32] We found that both the sizes of the creases and PBDT lattice patterns increase with the swelling time. That is, on short time scales (when swelling is independent of the

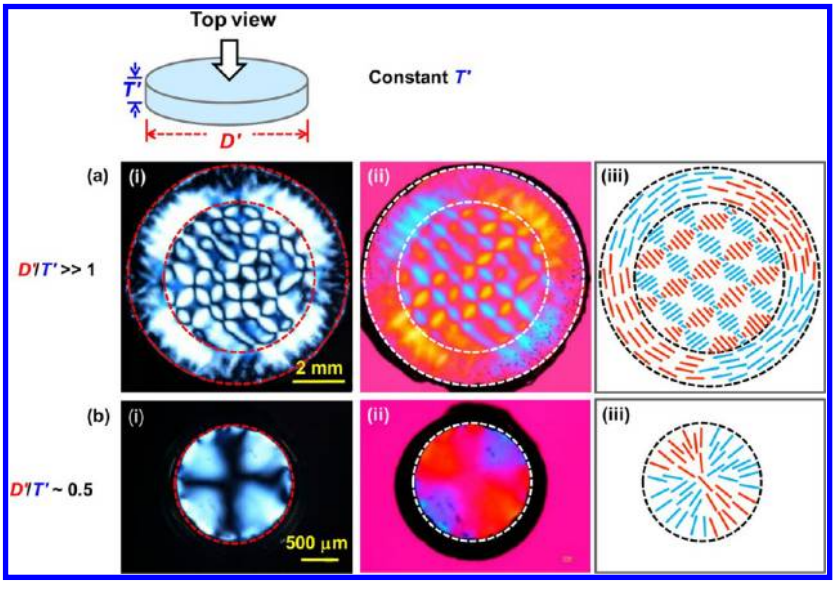


**Figure 6.** Ordered birefringent pattern and corresponding orientation of PBDT molecules formed in disc-shaped PDMAPAA-Q swollen hydrogel films with different diameters, $D'$. (a) $D'$ ∼ 8.4 mm, $T'$ ∼2 mm; (b) $D'$ ∼ 1 mm, $T'$ ∼2 mm. The left (i) and middle (ii) columns are POM images of the gels observed under crossed polarizers and with insertion of tint plate, respectively. In the POM image of part b(ii), the dark region beside the disc gel corresponds to some water existed between the gel and glass substrate, which results in strong light scattering. Illustrations in the right column (iii) indicate the PBDT molecular orientation in the hydrogel. Swelling ratio in length, $q$, of the gel is ∼2.2.


dx.doi.org/10.1021/ma401773w | *Macromolecules* 2013, 46, 9083–9090

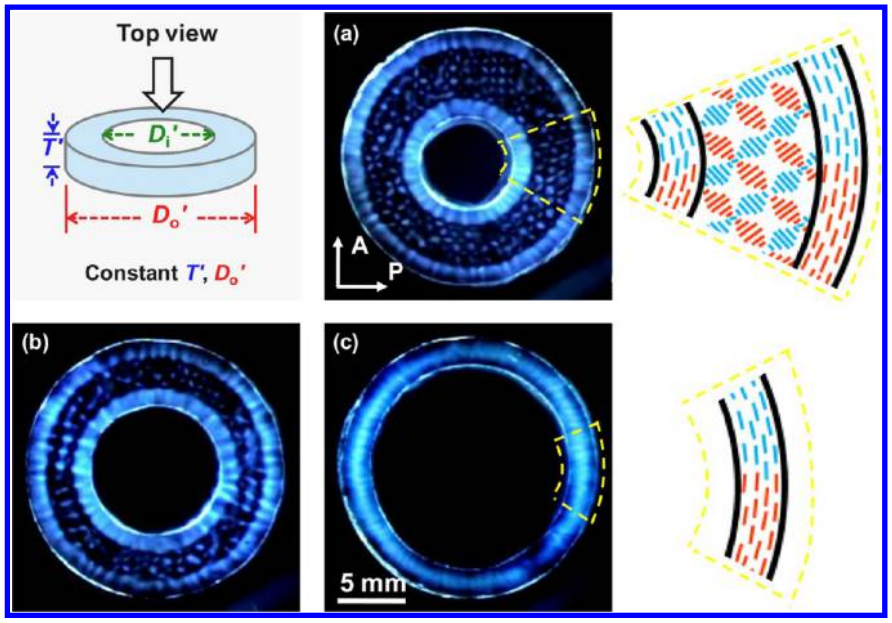


**Figure 7.** Ordered birefringent patterns observed under POM with corssed polarizers and the corresponding orientation of PBDT molecules in ring-shaped PDMAPAA-Q swollen hydrogels with constant thickness, $T' \sim 2$ mm, and outer diameter, $D_0' \sim 19$ mm, yet different inner diameter, $D_i'$: (a) $D_i' \sim 7$ mm, (b) $D_i' \sim 9$ mm, and (c) $D_i' \sim 15$ mm. Swelling ratio in length, $q$, of the gel is ~2.2.

dimensions and stress mismatches are greatest), the birefringence patterns do not depend on the overall geometry (the thickness) of the gel. However, the final largest size of the birefringence patterns that are "locked-in" the gel depends on the thickness of the swollen sample.

From the molecular orientations within swollen gel with a cuboid shape, we can see the significant geometric and edge effects on mechanical instabilities and PBDT alignments. Other complex structures could be developed in the swollen gels based on the same mechanism by cutting the as-prepared gel into other shapes and a subsequent fast swelling process. As shown in Figure 6a, the disk swollen gel with diameter, $D'$, much larger than gel thickness, $T'$, shows a similar birefringence pattern to that of cuboid gel. The central part of disk gel shows a lattice-like pattern; the edge part has concentric alignment of PBDTs, where molecules also align parallel to the boundary of disk gel.

When $D'$ decreases to a value comparable to $T'$, the disk gel shows quite different birefringence pattern and molecular alignment (Figure 6b). The entire disk swollen gel shows a Maltese cross. According to the birefringence colors, PBDTs form a radial structure; i.e., PBDTs align vertically to the gel boundary. This structure seems inconsistent with the previous results. However, it could also be explained by heterogeneous swelling induced internal stress and molecular orientations. During the swelling process, the disk gel could absorb water from the side, top, and bottom surfaces. When $D'$ is close to $0.5T'$, a strong swelling mismatch between the core region and the other outer "shell" region develops. If we look the gel as a cylinder, along the axial direction the outer region should expand more than the inner region, resulting in a concave region at the center of top and bottom surface. Therefore, a radial tensile stress is generated, leading to PBDTs orient in the radial direction which is frozen by the formation of polyion complexation.

If the as-prepared gels were cut into ring shape with outer and inner diameter, $D_0$ and $D_i$, respectively, the swollen gels also show complex birefringence patterns and molecular alignments. In Figure 7, $D_i'$ of the disc gel is gradually increased, yet $D_0'$ and $T'$ are kept constant. When $D_0' - D_i' > 4$ mm, the lattice-like pattern appears in the middle region of the ring, and a concentric alignment of PBDTs exists in the edges of ring. When $D_0' - D_i' \leq 3$ mm, lattice-like pattern disappears, the entire ring shows a uniform concentric structure of PBDTs. The essential pattern and molecular orientations in gels with ring shape are identical to those found in gels with a cuboid shape. This method is simple and universal to gels with other geometries to develop more complex structures of molecular alignments.

## CONCLUSION

In the present study, the orientation of the semirigid PBDT or its polyion complex is controlled by changing the shape and size of the synthesized PDMAPAA-Q hydrogel prior to the occurrence of free-fast-heterogeneous swelling. On the basis of the geometry and size of the as-prepared hydrogel, the internal stress field built by the fast swelling is of different kinds at the edge and central region of the hydrogels. Such heterogeneous distribution of internal stress induced by swelling leads to the creation of complex structures, including lattice-like structures, unidirectional or radial alignments of semirigid PBDTs, in hydrogels with specific shape and size. The transient internal stress induced molecular orientations are frozen by the polyion complexation formation during the swelling process. By changing the geometry and size of the hydrogel prior to swelling, the heterogeneously distributed internal stress can be tuned, permitting us to create more complex ordered structures within the gels. We have showed a facile method to develop structured hydrogels, and systematically studied the geometric and edge effects on tailoring the internal stress and thus molecular alignments. This work should merit designing other functional structured hydrogels and understanding the formation mechanism of various types of rich and intricate architectures of semirigid biomacromolecules in living soft tissues during their differential or nonequilibrium growth.

## ASSOCIATED CONTENT

### Supporting Information

POM images and plots of swelling ratios. This material is available free of charge via the Internet at http://pubs.acs.org.


dx.doi.org/10.1021/ma401773w | *Macromolecules* 2013, 46, 9083−9090

## AUTHOR INFORMATION


### Corresponding Author

*E-mail: (J.P.G.) gong@mail.sci.hokudai.ac.jp.

### Present Address

[§](Z.L.W.) Department of Polymer Science and Engineering, Zhejiang University, Hangzhou 310027, China.


### Notes

The authors declare no competing financial interest.

## ACKNOWLEDGMENTS

This research was financially supported by a Grant-in-Aid for Scientific Research (S) (No. 124225006) from Japan Society for the Promotion of Science (JSPS).

## REFERENCES


(1) Rossomando, E. F.; Alexander, S. *Morphogenesis: An Analysis of the Development of Biological Form*; Marcel Dekker Inc.: New York, 1992.
(2) Sharon, E.; Roman, B.; Marder, M.; Shin, G. S.; Swinney, H. L. *Nature* **2002**, *419*, 579.
(3) Hohlfeld, E.; Mahadevan, L. *Phys. Rev. Lett.* **2011**, *106*, 105702.
(4) Yin, J.; Gerling, G.; Chen, X. *Acta Biomater.* **2010**, *6*, 1487.
(5) Cerda, E.; Mahadevan, L. *Phys. Rev. Lett.* **2003**, *90*, 074302.
(6) Li, B.; Cao, Y.-P.; Feng, X.-Q.; Gao, H. *Soft Matter* **2012**, *8*, 5728.
(7) Yin, J.; Cao, Z.; Li, C.; Sheinman, I.; Chen, X. *Proc. Natl. Acad. Sci. U.S.A.* **2008**, *105*, 19132.
(8) Kucken, M.; Newell, A. C. *Europhys. Lett.* **2004**, *68*, 141.
(9) Liang, H.; Mahadevan, L. *Proc. Natl. Acad. Sci. U.S.A.* **2009**, *106*, 22049.
(10) Savin, T.; Kurpios, N. A.; Shyer, A. E.; Florescu, P.; Liang, H.; Mahadevan, L. *Nature* **2011**, *476*, 57.
(11) Nath, U.; Crawford, B. C. W.; Carpenter, R.; Coen, E. *Science* **2003**, *299*, 1404.
(12) Yin, J.; Chen, X.; Sheinman, I. *J. Mech. Phys. Solids* **2009**, *57*, 1470.
(13) Tanaka, T.; Sun, S.-T.; Hirokawa, Y.; Katayama, S.; Kucera, J.; Hirose, Y.; Amiya, T. *Nature* **1987**, *325*, 796.
(14) Tanaka, H.; Tomita, H.; Takasu, A.; Hayashi, T.; Nishi, T. *Phys. Rev. Lett.* **1992**, *68*, 2749.
(15) Klein, Y.; Efrati, E.; Sharon, E. *Science* **2007**, *315*, 1116.
(16) Barros, W.; de Azevedo, E. N.; Engelsberg, M. *Soft Matter* **2012**, *8*, 8511.
(17) Trujillo, V.; Kim, J.; Hayward, R. C. *Soft Matter* **2008**, *4*, 564.
(18) Guvendiren, M.; Yang, S.; Burdick, J. A. *Adv. Func. Mater.* **2009**, *19*, 3038.
(19) Kim, J.; Yoon, J.; Hayward, R. C. *Nat. Mater.* **2010**, *9*, 159.
(20) Ortiz, O.; Vidyasagar, A.; Wang, J.; Toomey, R. *Langmuir* **2010**, *26*, 17489.
(21) DuPont, S. J., Jr.; Cates, R. S.; Stroot, P. G.; Toomey, R. *Soft Matter* **2010**, *6*, 3876.
(22) Guvendiren, M.; Burdick, J. A.; Yang, S. *Soft Matter* **2010**, *6*, 5795.
(23) Dervaux, J.; Amar, M. B. *Annu. Rev. Condes. Matter Phys.* **2012**, *3*, 311.
(24) Wilson, R. H.; Smith, A. C.; Kačuráková, M.; Saunders, P. K.; Wellner, N.; Waldron, K. W. *Plant Physiol.* **2000**, *124*, 397.
(25) Kaunas, R.; Nguyen, P.; Usami, S.; Chien, S. *Proc. Natl. Acad. Sci. U.S.A.* **2005**, *102*, 15895.
(26) Stoclet, G.; Seguela, R.; Lefebvre, J. M.; Elkoun, S.; Vanmansart, C. *Macromolecules* **2010**, *43*, 1488.
(27) Wu, Z. L.; Sawada, D.; Kurokawa, T.; Kakugo, A.; Yang, W.; Furukawa, H.; Gong, J. P. *Macromolecules* **2011**, *44*, 3542.
(28) Shikinaka, K.; Koizumi, Y.; Kaneda, K.; Osada, Y.; Masunaga, H.; Shigehara, K. *Polymer* **2013**, *54*, 2489.
(29) Urayama, K.; Mashita, R.; Kobayashi, I.; Takigawa, T. *Macromolecules* **2007**, *40*, 7665.
(30) Kim, J.; Hanna, J. A.; Byun, M.; Santangelo, C. D.; Hayward, R. C. *Science* **2012**, *335*, 1201.
(31) Wu, Z. L.; Moshe, M.; Greener, J.; Therien-Aubin, H.; Nie, Z. H.; Sharon, E.; Kumacheva, E. *Nat. Commun.* **2013**, *4*, 1586.
(32) Arifuzzaman, M.; Wu, Z. L.; Kurokawa, T.; Kakugo, A.; Gong, J. P. *Soft Matter* **2012**, *8*, 8060.
(33) Vandenberg, E. J.; Diveley, W. R.; Filar, L. J.; Pater, S. R.; Barth, H. G. *J. Polym. Sci., Part A: Polym. Chem.* **1989**, *27*, 3745.
(34) Funaki, T.; Kaneko, T.; Yamaoka, K.; Oshedo, Y.; Gong, J. P.; Osada, Y.; Shibasaki, Y.; Ueda, M. *Langmuir* **2004**, *20*, 6518.
(35) Yang, W.; Furukawa, H.; Shigekura, Y.; Shikinaka, K.; Osada, Y.; Gong, J. P. *Macromolecules* **2008**, *41*, 1791.
(36) Wu, Z. L.; Arifuzzaman, M.; Kurokawa, T.; Le, K.; Hu, J.; Sun, T. L.; Furukawa, H.; Masunaga, H.; Gong, J. P. *Macromolecules* **2013**, *46*, 3581.
(37) Wu, Z. L.; Arifuzzaman, M.; Kurokawa, T.; Furukawa, H.; Gong, J. P. *Soft Matter* **2011**, *7*, 1884.
(38) Wu, Z. L.; Kurokawa, T.; Liang, S. M.; Furukawa, H.; Gong, J. P. *J. Am. Chem. Soc.* **2010**, *132*, 10064.
(39) Wu, Z. L.; Kurokawa, T.; Sawada, D.; Hu, J.; Furukawa, H.; Gong, J. P. *Macromolecules* **2011**, *44*, 3535.
(40) Holmes, D. P.; Roche, M.; Sinha, T.; Stone, H. A. *Soft Matter* **2011**, *7*, 5188.
(41) Mora, T.; Boudaoud, A. *Eur. Phys. J. E* **2006**, *20*, 119.
(42) Sultan, E.; Boudaoud, A. *J. Appl. Mech.* **2008**, *75*, 051002−1.
(43) Durning, C. J.; Morman, K. N., Jr. *J. Chem. Phys.* **1993**, *98*, 4275.
(44) Islam, M. F.; Nobili, M.; Ye, F.; Lubensky, T. C.; Yodn, A. G. *Phys. Rev. Lett.* **2005**, *95*, 148301.
(45) Wagner, K.; Harries, D.; May, S.; Kahl, V.; Rädler, J. O.; Ben-Shaul, A. *Langmuir* **2000**, *16*, 303.
(46) Gummel, J.; Cousin, F.; Boué, F. *J. Am. Chem. Soc.* **2007**, *129*, 5806.